

Semiannual Report

Atomic Layer Epitaxy Group IV Materials:
Surface Processes, Thin Films, Devices and
Their Characterization

DTIC
ELECTE
JUL 02 1992
S B D

Office of Naval Research
Supported under Grant #N00014-91-J-1416
Report for the period 1/1/92-6/1/92

Robert F. Davis, Salah Bedair*, Nadia A. El-Masry and Jeffrey T. Glass
Peter Goeller, Sean King, Joe Sumakeris, Lee Tye* and Wei Zhu
c/o Materials Science and Engineering Department
and *Electrical and Computer Engineering Department
North Carolina State University
Campus Box 7907
Raleigh, NC 27695-7907

DISTRIBUTION STATEMENT A

Approved for public release
Distribution Unlimited

June, 1992

92-17398



REPORT DOCUMENTATION PAGE

Form Approved
OMB No 0704 0188

Public reporting burden for this collection of information is estimated to average 1 hour per response, including the time for reviewing instructions, searching existing data sources, gathering and maintaining the data needed, and completing and reviewing the collection of information. Send comments regarding this burden estimate or any other aspect of this collection of information, including suggestions for reducing this burden, to Washington Headquarters Services, Directorate for Information Operations and Reports, 1215 Jefferson Davis Highway, Suite 1204, Arlington, VA 22202-4302, and to the Office of Management and Budget, Paperwork Reduction Project (0704-0188), Washington, DC 20503.

1. AGENCY USE ONLY (Leave Blank)

2. REPORT DATE
June 1992

3. REPORT TYPE AND DATES COVERED
Semiannual 1/1/92-6/30/92

4. TITLE AND SUBTITLE

Atomic Layer Epitaxy Group IV Materials: Surface Processes, Thin Films, Devices and Their Characterization

5. FUNDING NUMBERS

414v001---01
RA414
068342
2B

6. AUTHOR(S)

Robert F. Davis, Salah Bedair,
Nadia El-Masry and Jeffrey T. Glass

7. PERFORMING ORGANIZATION NAME(S) AND ADDRESS(ES)

North Carolina State University
Hillsborough Street
Raleigh, NC 27695

8. PERFORMING ORGANIZATION
REPORT NUMBER

N00014-91-J-1416

9. SPONSORING / MONITORING AGENCY NAME(S) AND ADDRESS(ES)

Office of the Chief of Naval Research
Electronics Division, Code 1114SS
800 North Quincy Street,
Arlington, VA 22217-5000

10. SPONSORING / MONITORING
AGENCY REPORT NUMBER

11. SUPPLEMENTARY NOTES

12a. DISTRIBUTION / AVAILABILITY STATEMENT

Approved for Public Release; Distribution Unlimited

12b. DISTRIBUTION CODE

13. ABSTRACT (Maximum 200 words)

Research concerned with the atomic layer epitaxy (ALE) of silicon carbide (SiC), diamond (C) and cerium dioxide (CeO₂) has been conducted within this reporting period. Equipment for the deposition of each of these materials, as well as experimental procedures for the conduct of the studies are in various stages of design, development and employment. Layer-by-layer deposition of Si and C from the precursors of Si₂H₆ and C₂H₄, respectively, and the resulting deposition of monocrystalline beta-SiC (100) has been achieved on Si(100) substrates. Rotation of the heated (820-980°C) sample under the individual source gases and a heated W filament located between these gases allowed a monolayer/cycle deposition to be achieved. Surface science related equipment and associated ultra-high vacuum systems are now being assembled to investigate and determine the chemical routes to achieve ALE of SiC by self-terminating chemical adsorption. Hexamethyldisilane species have been introduced into a hot filament CVD system in an attempt to nucleate diamond on an atomic scale on silicon substrate surfaces. The organosilicic layer formed was characterized by x-ray diffraction, Auger and x-ray photoelectron spectroscopies. The subsequent diamond nucleation and growth under various conditions was investigated. It is found that the nucleation density is very high under reverse dc biasing conditions. The structure of these particles is diamond-like in nature as revealed by Raman spectroscopy and scanning electron microscopy. A system is being constructed that will achieve atomic layer epitaxy of CeO₂ on silicon substrates. Operation in 1992 is anticipated.

14. SUBJECT TERMS

atomic layer epitaxy (ALE), Auger spectroscopy, cerium dioxide, diamond, forward scattering, silicon, silicon carbide, temperature programmed desorption, x-ray photoelectron spectroscopy

15. NUMBER OF PAGES

32

16. PRICE CODE

17. SECURITY CLASSIFICATION
OF REPORT

UNCLAS

18. SECURITY CLASSIFICATION
OF THIS PAGE

UNCLAS

19. SECURITY CLASSIFICATION
OF ABSTRACT

UNCLAS

20. LIMITATION OF ABSTRACT

SAR

Table of Contents

I. Introduction	1
References	2
II. Deposition of Silicon Carbide by Atomic Layer Epitaxy	4
A. Introduction	4
B. Experimental Procedure	4
C. Results	7
D. Discussion	11
E. Conclusions	13
F. Future Plans	13
G. References	13
III. Surface Science Investigations Related to the Atomic Layer Epitaxy of Silicon Carbide	14
A. Introduction	14
B. Experimental Procedure	14
1. Adsorption Kinetics and Temperature Programmed Desorption (TPD)	14
2. X-ray Photoelectron Spectroscopy (XPS) and Auger Electron Spectroscopy (AES)	15
C. Results	16
D. Discussion	16
E. Conclusions	18
F. Future Research Plans/Goals	18
G. References	18
IV. Atomic Layer Epitaxy of Diamond	19
A. Introduction	19
B. Experimental Procedure	19
1. Atomic Layer Epitaxy Chemistry of Diamond Deposition	19
2. Deposition of Organometallics	21
3. Substrates	22
4. Diamond Growth	22
C. Results and Discussion	23
1. Interlayer Structure	23
2. Diamond Growth	23
D. Conclusions	27
E. Future Research Plans/Goals	27
V. Epitaxial Growth of CeO₂ on Si	28
A. Introduction	28
B. Experimental Procedure	28
1. Silicon Wafer Cleaning	28
2. Thin Film Deposition	28
3. Characterization of Thin Films	29
C. Results	29
D. Discussion	30
E. Conclusions	31
F. Plans for Future Work	31
G. References	31
VI. Distribution List	32



For	
1	<input checked="" type="checkbox"/>
2	<input type="checkbox"/>
3	<input type="checkbox"/>
ten	
on/	
32	ity Codes
and/or	
special	
Dist	
A-1	

I. Introduction

Atomic layer epitaxy (ALE) is the sequential chemisorption of one or more elemental species or complexes within a time period or chemical environment in which only one monolayer of each species is chemisorbed on the surface of the growing film in each period of the sequence. The excess of a given reactant which is in the gas phase or only physisorbed is purged from the substrate surface region before this surface is exposed to a subsequent reactant. This latter reactant chemisorbs and undergoes reaction with the first reactant on the substrate surface resulting in the formation of a solid film. There are essentially two types of ALE which, for convenience, shall be called Type I and Type II.

In its early development in Finland, the Type I growth scenario frequently involved the deposition of more than one monolayer of the given species. However, at that time, ALE was considered possible only in those materials wherein the bond energies between like metal species and like nonmetal species were each less than that of the metal-nonmetal combination. Thus, even if multiple monolayers of a given element were produced, the material in excess of one monolayer could be sublimed by increasing the temperature and/or waiting for a sufficient period of time under vacuum. Under these chemical constraints, materials such as GaAs were initially thought to be improbable since the Ga-Ga bond strength exceeds that of the GaAs bond strength. However, the self-limiting layer-by-layer deposition of this material proved to be an early example of type II ALE wherein the trimethylgallium (TMG) chemisorbed to the growing surface and effectively prevented additional adsorption of the incoming metalorganic molecules. The introduction of As, however caused an exchange with the chemisorbed TMG such that a gaseous side product was removed from the growing surface. Two alternating molecular species are also frequently used such that chemisorption of each species occurs sequentially and is accompanied by extraction, abstraction and exchange reactions to produce self-limiting layer-by-layer growth of an element, solid solution or a compound.

The type II approach has been used primarily for growth of II-VI compounds [1-13]; however, recent studies have shown that it is also applicable for oxides [14-18], nitrides [19], III-V GaAs-based semiconductors [20-33] and silicon [34-36]. The advantages of ALE include monolayer thickness control, growth of abrupt interfaces, growth of uniform and graded solid solutions with controlled composition, reduction in macroscopic defects and uniform coverage over large areas. A commercial application which makes use of the last attribute is large area electroluminescent displays produced from II-VI materials. Two comprehensive reviews [37,6], one limited overview [38] and a book [39] devoted entirely to the subject of ALE have recently been published.

The materials of concern in this program include silicon carbide (SiC), diamond (C) and cerium dioxide (CeO₂). Equipment for the ALE deposition of each of these materials, as well as the experimental procedures for the conduct of these studies are in various stages of design,

development and employment. The following sections introduce each topic, detail the experimental approaches, report the results to date and provide a discussion and a conclusion for each material. Each major section is self-contained with its own figures, tables and references.

References

1. T. Suntola and J. Antson, U.S. Patent 4,058,430 (1977).
2. M. Ahonen, M. Pessa and T. Suntola, *Thin Solid Films*, **65**, 301 (1980).
3. M. Pessa, R. Makela, and T. Suntola, *Appl. Phys. Lett.*, **38**, 131 (1981).
4. T. Yao and T. Takeda, *Appl. Phys. Lett.*, **48**, 160 (1986).
5. T. Yao, T. Takeda, and T. Watanuki, *Appl. Phys. Lett.*, **48**, 1615 (1986).
6. T. Yao, *Jpn. J. Appl. Phys.*, **25**, L544 (1986).
7. T. Yao and T. Takeda, *J. Cryst. Growth*, **81**, 43 (1987).
8. M. Pessa, P. Huttunen and M.A. Herman, *J. Appl. Phys.*, **54**, 6047 (1983).
9. C.H.L. Goodman and M.V. Pessa, *J. Appl. Phys.*, **60**, R65 (1986).
10. M.A. Herman, M. Valli and M. Pessa, *J. Cryst. Growth*, **73**, 403 (1985).
11. V.P. Tanninen, M. Oikkonen and T. Tuomi, *Phys. Status Solidi*, **A67**, 573 (1981).
12. V.P. Tanninen, M. Oikkonen and T. Tuomi, *Thin Solid Films*, **90**, 283 (1983).
13. D. Theis, H. Oppolzer, G. Etchinghaus and S. Schild, *J. Cryst. Growth*, **63**, 47 (1983).
14. S. Lin, *J. Electrochem. Soc.*, **122**, 1405 (1975).
15. H. Antson, M. Leskela, L. Niinisto, E. Nykanen and M. Tammenmaa, *Kem.-Kemi*, **12**, 11 (1985).
16. R. Tornqvist, Ref. 57 in the bibliography of Chapt. 1 of Ref. 39 of this proposal.
17. M. Ylilammi, M. Sc. Thesis, *Helsinki Univ. of Technology*, Espoo (1979).
18. L. Hiltunen, M. Leskela, M. Makela, L. Niinisto, E. Nykanen and P. Soininen, *Surface Coatings and Technology*, in press.
19. I. Suni, Ref. 66 in the bibliography of Chapt. 1 of Ref. 39 in this report.
20. S.M. Bedair, M.A. Tischler, T. Katsuyama and N.A. El-Masry, *Appl. Phys. Lett.*, **47**, 51 (1985).
21. M.A. Tischler and S.M. Bedair, **48**, 1681 (1986).
22. M.A. Tischler and S.M. Bedair, *J. Cryst. Growth*, **77**, 89 (1986).
23. M.A. Tischler, N.G. Anderson and S.M. Bedair, *Appl. Phys. Lett.*, **49**, 1199 (1986).
24. M.A. Tischler, N.G. Anderson, R.M. Kolbas and S.M. Bedair, *Appl. Phys. Lett.*, **50**, 1266 (1987).
25. B.T. McDermott, N.A. El-Masry, M.A. Tischler and S.M. Bedair, *Appl. Phys. Lett.*, **51**, 1830 (1987).
26. M.A. Tischler, N.G. Anderson, R.M. Kolbas and S.M. Bedair, *SPIE Growth Comp. Semicond.*, **796**, 170 (1987).
27. S.M. Bedair in *Compound Semiconductor Growth Processing and Devices for the 1990's*, Gainesville, FL, 137 (1987).
28. J. Nishizawa, H. Abe and T. Kurabayashi, *J. Electrochem. Soc.*, **132**, 1197 (1985).
29. M. Nishizawa, T. Kurabayashi, H. Abe, and N. Sakurai, *J. Electrochem. Soc.*, **134**, 945 (1987).
30. P.D. Dapkus in Ref. 27, p. 95.
31. S.P. Denbaars, C.A. Beyler, A. Hariz and P.D. Dapkus, *Appl. Phys. Lett.*, **51**, 1530 (1987).
32. M. Razeghi, Ph. Maurel, F. Omnes and J. Nagle, *Appl. Phys. Lett.*, **51**, 2216 (1987).
33. M. Ozeki, K. Mochizuki, N. Ohtsuka and K. Kodama, *J. Vac. Sci. Technol.* **B5**, 1184 (1987).
34. Y. Suda, D. Lubben, T. Motooka and J. Greene, *J. Vac. Sci. Technol.*, **B7**, 1171 (1989).
35. J. Nishizawa, K. Aoki, S. Suzuki and K. Kikuchi, *J. Cryst. Growth*, **99**, 502 (1990).

36. T. Tanaka, T. Fukuda, Y. Nagasawa, S. Miyazaki and M. Hirose, *Appl. Phys. Lett.*, **56**, 1445 (1990).
37. T. Suntola and J. Hyvarinen, *Ann. Rev. Mater. Sci.*, **25**, 177 (1985).
38. M. Simpson and P. Smith, *Chem. Brit.*, **23**, 37 (1987).
39. T. Suntola and M. Simpson, *Atomic Layer Epitaxy*, Chapman and Hall, New York, 1990.

II. Deposition of Silicon Carbide by Atomic Layer Epitaxy

A. Introduction

The extremes in the thermal, mechanical, chemical, and electronic properties of all the common polytypes of SiC allow the types and the numbers of current and conceivable applications of this material to be substantial. From an electronics viewpoint, it possesses a range of wide band gaps [1] at 300 K, e.g., 2.2 eV (3C), 2.86 eV (6H) and 3.3 eV (2H); as well as high values of saturated electron drift velocity of 2×10^7 cm/s (6H) [2] (a slightly higher value has been predicted [3] for 3C (beta) because of reduced phonon scattering); junction breakdown electric field (5×10^6 V/cm [4] and thermal conductivity (3.5 W/cm°C at 300 K) [5]. As such, the primary driving forces for the current interest in SiC for electronic devices are its capabilities for high-power, -speed, -temperature, and light-emitting devices resistant to radiation damage. Discrete devices having these properties have been achieved and characterized in the laboratory.

The high thermal conductivity of SiC also indicates the potential for high density integration of SiC devices. The idea has received considerable impetus with the recent development and scale-up of the seed-sublimation growth technique for producing commercially viable single crystal a (6H)-SiC boules from which highly thermally conductive wafers are obtained. Significant advances have also been made in the growth of monocrystalline beta and alpha (6H) thin films via chemical vapor deposition (CVD) and the incorporation of n- and p-type dopants into these films during deposition or via ion implantation.

The objective of this research is to extend the state-of-the-art regarding SiC thin films via the employment of atomic layer epitaxy (ALE) to deposit the material on selected substrates and eventually to fabricate devices using this method. The following subsections describe the experimental procedures and discuss the results and conclusions of the research conducted in this reporting period.

B. Experimental Procedure

Figure 1 shows the basic internal components of the ALE system growth chamber including the vane assembly which separates the gases. The fabrication and employment of this reactor was discussed in the previous report (December 31, 1991).

In this reactor, the substrates rest on a heated platform and rotate between fluxes of Si_2H_6 and C_2H_4 as depicted in Figure 1. The samples pause beneath intermediate zones which contain hot tungsten filaments that are used to aid in surface migration of the deposited Si and C species.

Heteroepitaxial films deposited on (001) Si substrates oriented 3° off-axis toward the [011] pole have been analyzed on the basis of composition, crystallinity, growth per cycle, and

morphology using depth profiling Auger, RHEED, ellipsometry and TEM. Growth rate, as measured by ellipsometry corresponds to approximately 1 monolayer per cycle. Both highly textured polycrystalline and single crystal films of β -SiC have been deposited. The potential for the growth of monocrystalline films improves significantly with extended residence time beneath the filament.

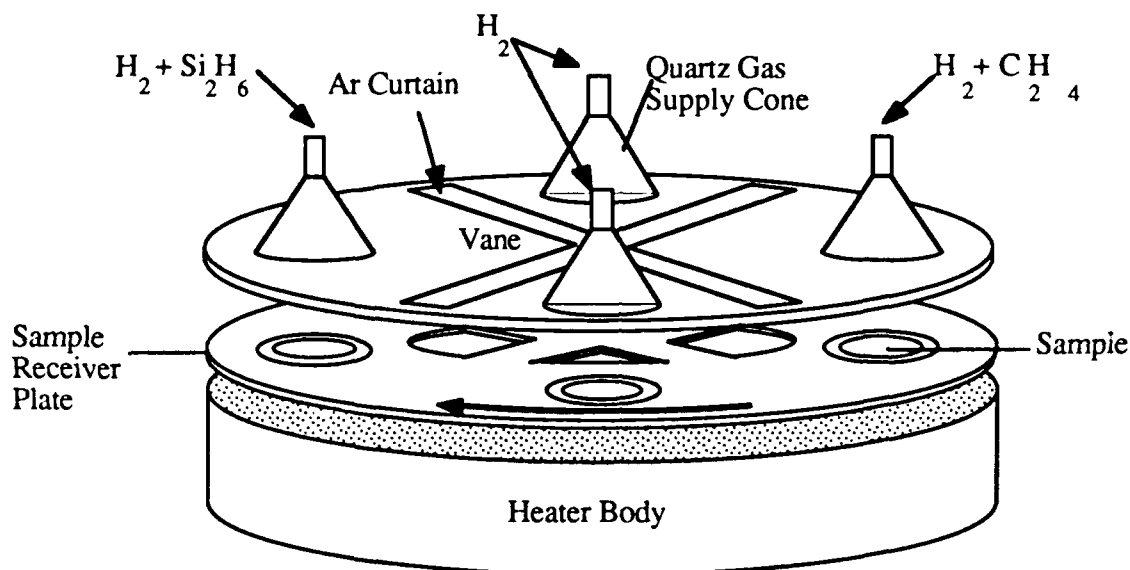


Figure 1. Internal components of ALE deposition system.

A typical run follows the experimental procedure described by Table I. The Si_2H_6 pre-exposure is based on the method of Kunii and Sakakibara [1] in which the surface of the Si substrate is exposed to a low partial pressure of a silicon source gas such as Si_2H_6 at $\sim 950^\circ\text{C}$ to efficiently remove any oxide. Furthermore, this preliminary Si_2H_6 exposure will deposit a homoepitaxial Si film which is expected to be of better quality than the original silicon substrate and should improve the quality of the subsequent heteroepitaxial silicon carbide film.

Films have been grown across a broad range of process variables as detailed in Table II. While most films during this reporting period have been highly textured polycrystalline, we have recently achieved single crystal SiC films on Si at 850°C by omitting the preliminary carburization step.

As the ALE system contains no in situ analytical capacity the samples must be removed and transported elsewhere for analysis. The analytical techniques employed include SEM, TEM, depth profiling Auger, ellipsometry, and RHEED. For clearer RHEED images, the samples are heated to 900°C in high vacuum to remove the native oxide before analysis. This step does not alter the RHEED image, but only reduces the background brightness.

Initial growth and characterization results are presented in the following subsections, and discussion for both the poly- and monocrystalline films.

Table I. Experimental Procedure

- The sample is (100) Si oriented off axis 3° toward <011>.
 - Clean the sample using the standard RCA procedure and load into system immediately.
 - Transfer into ALE chamber once vacuum is $< 10^{-7}$ torr.
 - Start H₂ and Ar gas flow.
 - Ramp up to growth temperature at 10° C per minute.
 - Wait under H₂ for 3 minutes at growth temperature.
 - Start Si₂H₆ flow.
 - Rotate sample under Si₂H₆ for 5 revolutions.
 - Stop sample under H₂.
 - Start C₂H₄ flow.
 - Turn on filament.
 - Start sample rotation, typically rotate 360° and pause under the filament for 30 seconds, repeating as required.
 - Once rotation is finished, turn off Si₂H₆ and C₂H₄.
 - Decrease temperature to $< 300^{\circ}\text{C}$.
 - Turn off all gasses and evacuate to high vacuum.
 - Remove the sample through load lock.
-
-

Table II. Ranges of Process Variables

Sample temperature:	820° C – 980° C
Si ₂ H ₆ flow:	0.2 to 10 sccm in 0; 75 to 300 sccm of H ₂
C ₂ H ₄ flow:	1.5 to 20 sccm in 0; 75 to 200 sccm of H ₂
Filament temperature:	25° C; 1450° C to 1700° C
Time per revolution:	0.66 to 10 seconds per revolution
Residence time under: filament	0 to 60 seconds

C. Results

The initial SiC films produced in this research were randomly oriented polycrystalline β -SiC. By reducing the supply rate of reactants to the sample, extremely well oriented films were achieved. Finally, by allowing a substantial pause time below the hot filament between each exposure to C_2H_4 and Si_2H_6 , single crystal films of β -SiC have been deposited.

Auger depth profiling and spot analysis for a SiC film is seen in Figures 2 and 4, respectively. Auger performed on the films reveals a very constant stoichiometric SiC film with no detectable O within the film, as seen in Figure 4. Similar depth profiling and spot Auger results for analysis of a SiC wafer standard are presented in Figures 3 and 5, respectively for comparison.

There is a significant influence of pause time below the filaments on the degree of preferred orientation of the polycrystalline SiC films as pictured in Figure 6. All four samples were run under similar conditions: sample temperature of $970^\circ C$, Si_2H_6 flow rate of 3 sccm in 75 sccm of H_2 , C_2H_4 flow rate of 7.5 sccm in 75 sccm of H_2 , filament at $1650^\circ C$, 10 seconds per revolution, exposure to each gas stream for 2.5 seconds, and 50 revolutions total. The only variable was the pause time below the filament as detailed.

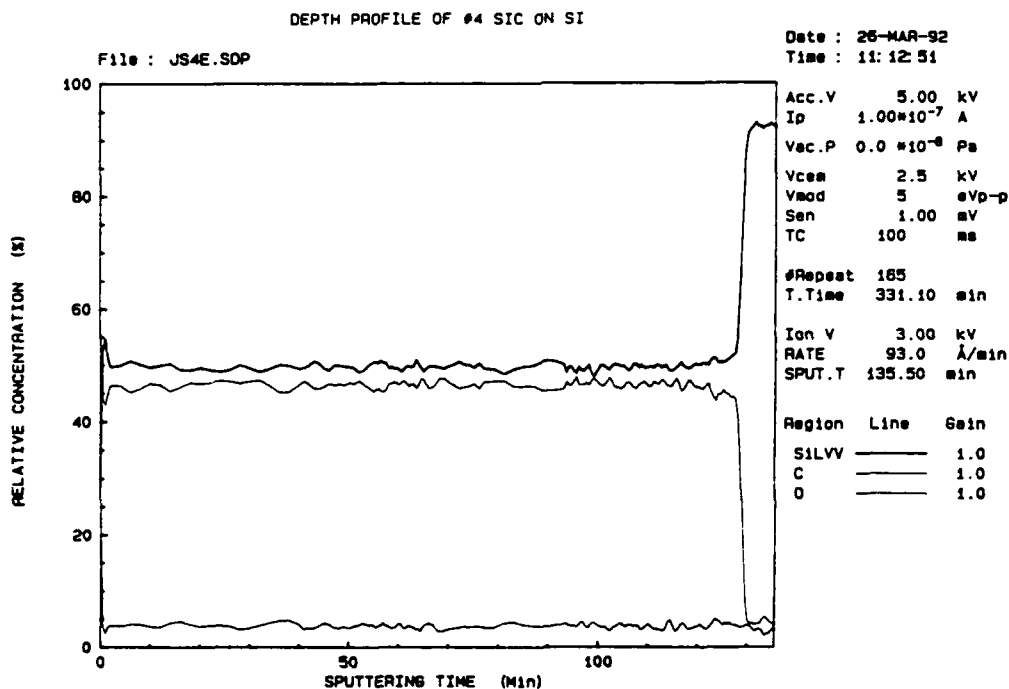


Figure 2. Auger depth chemical profile of polycrystalline film. Growth conditions: sample temperature of $900^\circ C$, Si_2H_6 flow rate of 3 sccm in 150 sccm of H_2 , C_2H_4 flow rate of 20 sccm in 150 sccm of H_2 , continuous rotation at 5 rpm for 700 revolutions, with filament at $1400^\circ C$.

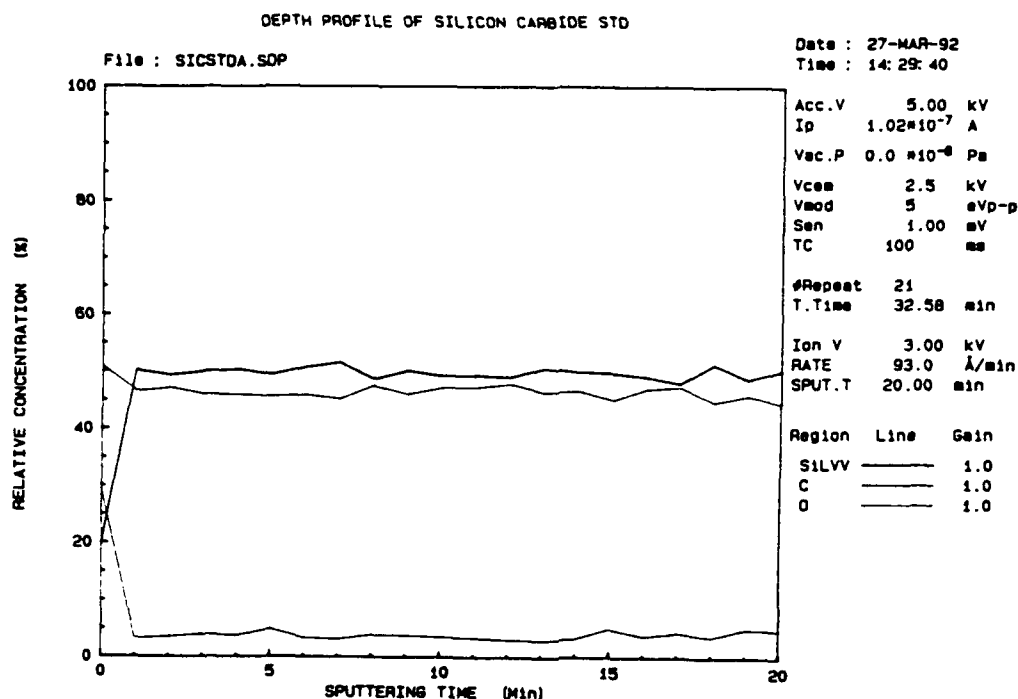


Figure 3. Auger depth chemical profile of a (6H) SiC wafer from boule grown by Cree Research, Inc., Durham, NC.

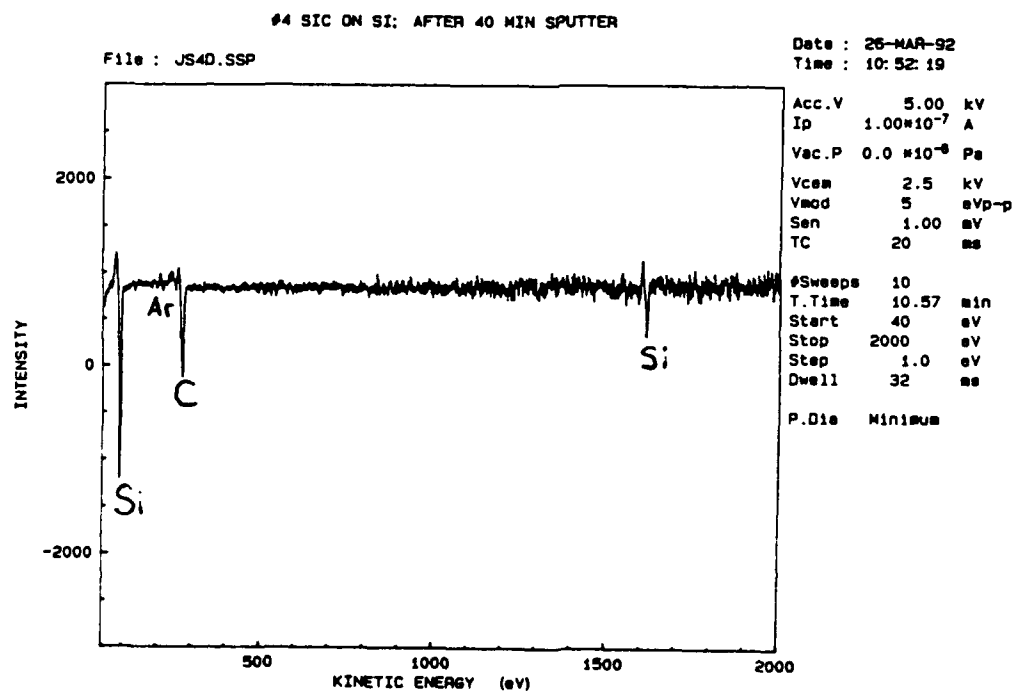


Figure 4. Auger spot chemical analysis of polycrystalline film. Growth conditions: sample temperature of 900°C, Si₂H₆ flow rate of 3 sccm in 150 sccm of H₂, C₂H₄ flow rate of 20 sccm in 150 sccm of H₂, continuous rotation at 5 rpm for 700 revolutions, with filament at 1400 °C.

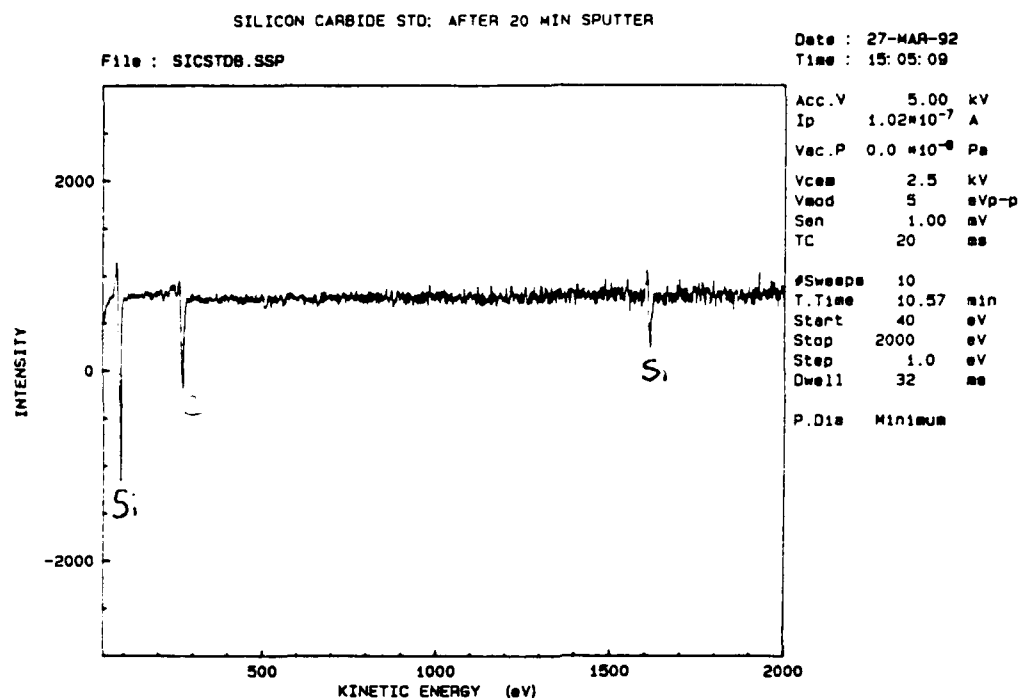


Figure 5. Auger spot chemical analysis of a (6H) SiC wafer from boule grown by Cree Research, Inc., Durham, NC.

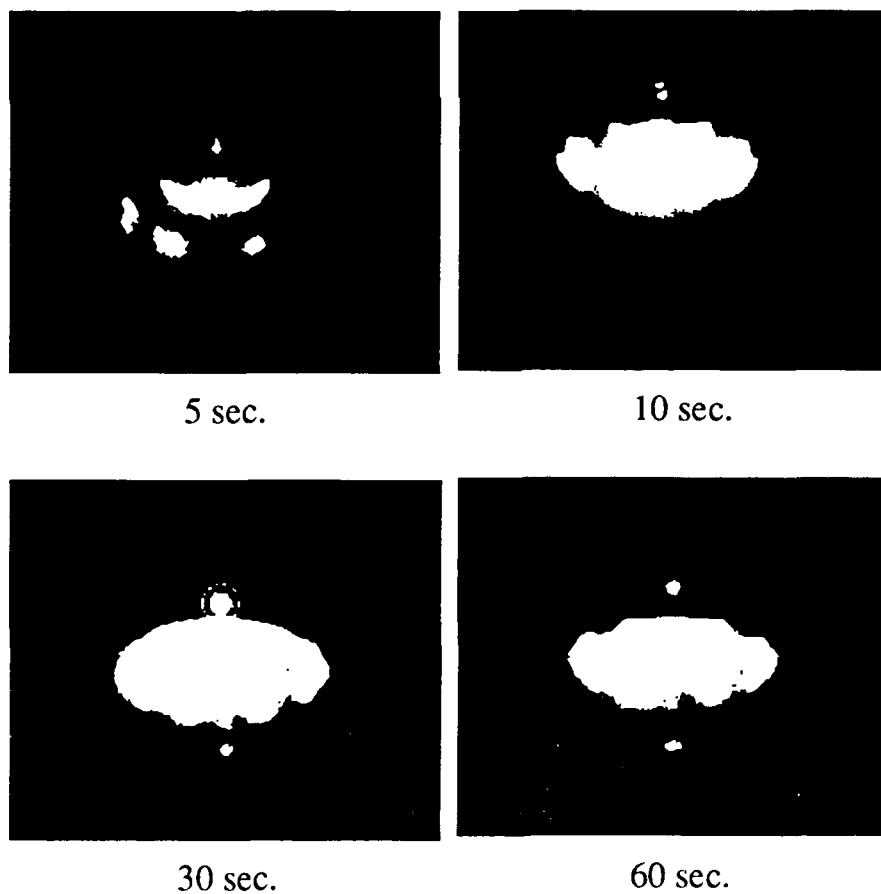


Figure 6. Improvement in the degree of preferred orientation with residence time below the tungsten filament.

It can be seen in the previous figure that the preferred orientation of the film improves greatly with the residence time below the filament up to a maximum residence of 30 seconds beyond which little further improvement occurs. The temperature rise of the sample below the filament is difficult to measure, but by optical pyrometry, it is of the order of 100°C. The thickness of all four films as measured by ellipsometry was $\approx 265\text{\AA} \pm 15\text{\AA}$. As the thickness varies by 6% while the length of the runs varies by a factor 12, there is good gas separation in the reactor.

Attempts to employ the Si_2H_6 pre-exposure invariably resulted in polycrystalline SiC films, although the deposited Si film was completely crystalline. The difficulty arises because the process involved in the deposition of the Si film generated a high concentration of pits at the surface which resulted in the subsequent SiC film nucleating heterogeneously within these pits and finally forming a polycrystalline SiC film. Therefore the preliminary Si film must not only be single crystal, but also very smooth.

Single crystal films of SiC have been grown only when the Si_2H_6 pre-exposure is not employed. Figure 7 shows the RHEED patterns for a single crystal film of SiC. The growth conditions were: sample temperature of 850°C, Si_2H_6 flow rate of 0.8 sccm in 300 sccm of H_2 , C_2H_4 flow rate of 2.0 sccm in 200 sccm of H_2 , filament temperature of 1600°C, 10 seconds per revolution, exposure to each process gas for 2.5 seconds, pause time below the filament for 30 seconds, and 50 revolutions total.

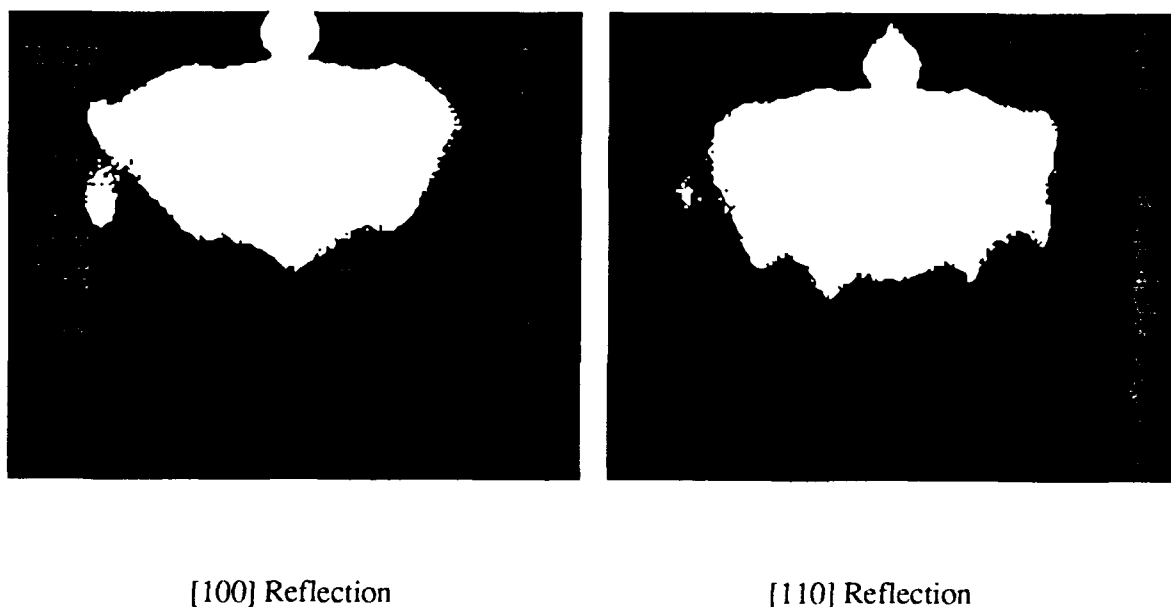


Figure 7. RHEED patterns for monocrystalline SiC film deposited at 850°C.

The film in Figure 7 is 107Å thick, corresponding to a growth of β -SiC at ~ 1 monolayer per cycle. Repeating the above run without using the filament resulted in the deposition of a in polycrystalline film.

D. Discussion

The philosophy employed in this research is to expose the heated substrate or growing SiC film to a Si_2H_6 flux that is equivalent to approximately 1 monolayer of Si. It is reported that at the temperatures used in this work, Si_2H_6 will decompose quickly on a Si surface resulting in adsorbed SiH_2 fractions which form a Si film through the evolution of H_2 [7,8] The Si terminated substrate is then rotated to a zone supplying C_2H_4 which will react with the adsorbed Si. It is believed at this time that the reaction of ethylene with the Si ad atoms on the deposited SiC film is self terminating. Haq and Learn[9] have reported that no reaction of C_2H_2 occurs on a SiC substrate at 920°C , but that this hydrocarbon reacts readily with exposed Si under the same conditions. Following this operation, the samples are allowed to remain under a hot filament to desorb any H atoms that remain bound to the carbon species fragments forming the film and to enhance the migration of the adsorbed C to growth steps. This latter process assists in the achievement of a single crystal film. After each pause, the rotation resumes to grow a subsequent layer of SiC.

The filament has a marked effect on the crystallinity of the deposited film. Under some conditions its use makes the difference between the deposition of single crystal and polycrystalline films. At a sample temperature of 970°C , the improvement of the film by pausing under the filament peaks after approximately a 30 second residence time during which the position of the sample is 0.5 cm. below the 1650°C filament

The optimal growth conditions favor a very dilute supply of Si_2H_6 , extended residence time below the filament, and a sample temperature of less than 980°C . The preference for a dilute supply of Si_2H_6 can be explained by considering that the C_2H_4 supplied after the Si_2H_6 will only deposit on exposed Si, therefore if more than one monolayer of Si is deposited insufficient C will deposit, following this logic, better films may be deposited if the Si_2H_6 exposure is less than the equivalent of 1 monolayer. Extended residence time below the filament will both aid in surface mobility which will improve crystallinity, and enhance the reaction of the deposited C_2H_4 fractions. The preference for lower sample temperature is harder to justify except for considering the substrate surface.

Pitting of Si at elevated temperatures has been observed in our samples, especially those where a pre-exposure of Si_2H_6 was conducted. The nucleation of the SiC film is very favorable within and on the high energy edges of these pits. However once a portion of the film grows away from a given pit, it may be misaligned with other sections of the growing film, which will give rise to polycrystallinity. Reisman has studied the thermal pitting of Si

[10] and suggests that at lower temperatures (900°-1000°C), surface heterogeneities such as dislocations, impurities, and defects in a native oxide drive pitting. As the wafers employed are off axis, the surface defect concentration will be enhanced, and this may be responsible for the excessive pitting. In addition to lattice defects, a discontinuous native oxide may be responsible for the pitting, implying that better sample preparation is required.

A preferred method of cleaning the sample within the reactor would be a Si_2H_6 pre-exposure which has been shown to remove oxide[6], and which should generate a better surface for heteroepitaxy than the original substrate surface. To do this without pitting the substrate we will need to begin at lower temperatures. Kunii and Sakakibara report that the cleaning by Si_2H_6 is effective at a temperature as low 850°C. Smith and Ghidini [11] have defined conditions, where at a given vapor pressure of O, there is a minimum Si substrate temperature above which any O incident upon the surface will form volatile SiO which will desorb, leaving a clean Si surface, and below which stable SiO_2 will form. The conditions for (100) Si are depicted in Figure 8.

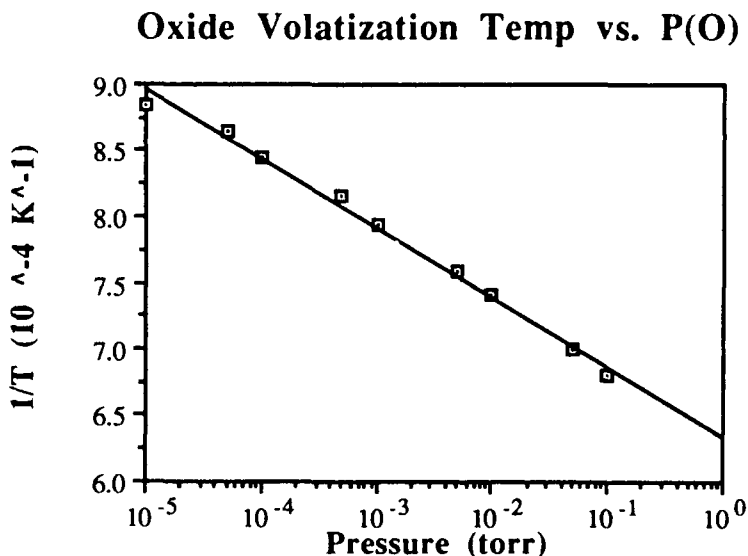


Figure 8. Minimum temperature to form volatile SiO on (100) Si.

For the process involved in this research, and the purity of the gases, the background of O as either O_2 or H_2O during processing will be about 5×10^{-7} torr. We have fit a curve to the data of Smith and Ghidini. The related equation is:

$$1/T_{\min} (10^{-4} \text{ K}^{-1}) = 6.3426 - 0.52497 \times \text{LOG} [P(\text{O}_2)]$$

with a correlation of 0.993. Applying 5×10^{-7} torr to the fit gives $T_{\min} = 763^{\circ}\text{C}$. Therefore cleaning at 850°C should produce a clean Si surface that would persist.

E. Conclusions

Single crystal and polycrystalline films of β -SiC have been grown on Si substrates at temperatures as low as 850°C . The quality of the films is strongly dependent on residence below a hot filament.

The deposited films are defective by TEM inspection, and substantial improvement is required. The primary cause for the low film quality is probably pitting of the substrate. To minimize this, a low temperature pre exposure to Si_2H_6 should help remove any contaminants or surface oxide encouraging pitting and provide an improved surface for heteroepitaxy. After a thoroughly cleaned substrate is achieved, higher growth temperatures may be employed without causing the excessive pitting previously observed and resulting in better SiC films.

F. Future Plans

1. Perform an experimental series to determine what role the filament plays in the deposition of SiC. The series will involve substituting argon for hydrogen used as a diluent gas.
2. Perform an experimental series to determine the effect of exposure of Si_2H_6 in sub-monolayer dosages for each cycle on the crystallinity of the films.
3. Determine whether reaction of C_2H_4 with Si ad atoms is self-terminating.
4. Develop the ability to grow smooth homoepitaxial single crystal films of Si as the initial layer on which to deposit the SiC

G. References

1. N. W. Jepps and T. F. Page, "Polytypic transformations in silicon carbide," in *Progress in Crystal Growth and Characterization, Vol. 8 - Crystal Growth and Characterization of Polytype Structures*, P. Krishna, Ed., Pergamon, NY, 1983, pp. 259-307.
2. W. von Muench and E. Pettenpaul, *J. Appl. Phys.* **48** 4823 (1977).
3. P. Das and D. K. Ferry, *Solid-State Electron.* **19** 851 (1976)
4. W. von Muench and I. Pfaffender, *J. Appl. Phys.* **48** 4831 (1977)
5. E. A. Bergemeister, W. von Muench, and E. Pettenpaul, *J. Appl. Phys.* **50** 5790 (1979)
6. Y. Kunii and Y. Sakakibara, *Jpn. J. Appl. Phys.* **26** 1816 (1987)
7. J. L. Regolini, D. Bensahel, and J. Mercier, *J. Electron. Mater.* **19** 1075 (1990)
8. J. J. Boland, *Physical Review B* **44** 1383 (1991)
9. K. E. Haq, and A. J. Learn, *J. Appl. Phys.* **40** 431 (1968)
10. A. Reisman, D. Temple and P. L. Smith, *J. Electrochem Soc.* **137** 284 (1990)
11. F. W. Smith and G. Ghidini, *J. Electrochem. Soc.* **129** 1300 (1982)

III. Surface Science Investigations Related to the Atomic Layer Epitaxy of Silicon Carbide

A. Introduction

Previous reports have proposed the chemistry believed necessary for the deposition of SiC by ALE. This proposed deposition mechanism was based on previous surface chemistry studies of Si₂H₆ on Si [1-4] and C₂H₄ on Si [5,6]. Unfortunately, these studies considered only the independent adsorption of each species on silicon. These studies did not address at the subsequent adsorption of a second species on top of the first adsorbed species, i.e. the adsorption of C₂H₄ on top of Si₂H₆. In order to better understand the chemistry necessary for the deposition of SiC by ALE using C₂H₄ and Si₂H₆ as precursor species, these surface chemistry studies must be expanded to include the subsequent adsorption of another species. Such studies will provide insight into the true nature of the monolayer by monolayer deposition mechanism of SiC.

The objective of- this research is to extend these surface chemistry studies important to the ALE of SiC by including the subsequent adsorption of a second precursor specie. These studies will include the study of the surface adsorption and chemical reaction kinetics of Si₂H₆ and C₂H₄ on silicon, C₂H₄ on Si₂H₆ adsorbed on Si, and Si₂H₆ on C₂H₄ adsorbed on Si. An ultra high vacuum (UHV) system containing a variety of analytical tools is currently being designed for these studies. The vacuum system will be comprised of two chambers with several analytical techniques which include: adsorption kinetics experiments, temperature programmed desorption (TPD), X-ray photoelectron spectroscopy (XPS), Auger electron spectroscopy (AES), and X-ray photoelectron/Auger electron forward scattering experiments. It will be joined to another vacuum system containing low energy electron diffraction and ultra-violet spectroscopy. The following subsections discuss and describe in more detail the UHV system and the associated analytical techniques.

B. Experimental Procedure

1. Adsorption Kinetics and Temperature Programmed Desorption (TPD)

The first of two UHV chambers will incorporate the equipment necessary for kinetics of adsorption studies and temperature programmed desorption. A multipurpose quadrupole mass spectrometer (QMS) detector design by Prof. John T. Yates, Jr., of the University of Pittsburgh (with whom we are collaborating on this research) will be used to perform both types of experiments [7]. The multipurpose QMS design consists of a QMS from Hiden Analytical Ltd. encased in a specially designed apertured chamber. The QMS chamber includes both an aperture for line of sight desorption detection as well as a fitted closure for random flux detection. This configuration allows for a variety of measurements to be made such as: absolute

surface coverage determination, absolute sticking probability as a function of surface coverage, and line of sight thermal desorption [7].

Using the above mentioned apparatus, the adsorption of Si_2H_6 on C_2H_4 adsorbed on Si and vice versa will be studied. Initial studies for calibration purposes will focus on duplicating the studies of the independent adsorption of C_2H_4 and Si_2H_6 on Si. These studies will then quickly turn to the investigation of the sticking probability and saturation surface coverage of Si_2H_6 on C_2H_4 adsorbed Si and vice versa. These experiments will also employ a microcapillary array-molecular beam doser design also by Dr. John T. Yates, Jr. [8,9]. This doser design will be used due to its capability to reduce wall effects and provide a highly collimated beam of gas which represents a relatively small load to the UHV system. Temperature programmed desorption of C_2H_4 and Si_2H_6 adsorbed on one another on silicon will also be performed in order to determine the thermal stability of each species on the surface and also the species activation energy for desorption.

2. X-ray Photoelectron Spectroscopy (XPS) and Auger Electron Spectroscopy (AES)

The second UHV chamber will incorporate the equipment necessary for x-ray photoelectron spectroscopy and AES experiments. These experiments will be performed together with the adsorption kinetics/TPD experiments to enhance the information gained from both. X-ray photoelectron spectroscopy and AES will be used to provide information on the chemical composition of the silicon surfaces after exposures to various doses of C_2H_4 and Si_2H_6 . The chemical shift data provided by XPS will be used to determine the type of bonding between the C_2H_4 and Si_2H_6 species and the bonding between the species and the silicon surface. AES will be primarily used to provide information on the relative concentrations of different elements at the silicon surface.

In addition to standard XPS and AES, a third analytical technique, namely, X-ray photoelectron/Auger electron forward scattering will be performed with the AES-XPS equipment. The theory and application of this technique has been reviewed recently by Egelhoff [10]. It is based on some of the subtleties of the XPS and AES techniques. Specifically, the intensity of the emitted XPS or Auger electrons is measured as function of the exit angle of the electrons from the surface. Electrons emitted by an atom in an XPS or Auger process are strongly forward scattered by the potential of other surrounding atoms. This forward scattering produces enhanced intensities along internuclear axes or bond directions thus giving bond angles and some structural information. This technique will therefore be used to elucidate structural information on how C_2H_4 and Si_2H_6 adsorb to the clean Si surface and the $\text{C}_2\text{H}_4/\text{Si}_2\text{H}_6$ saturated surfaces.

As mentioned previously, XPS, AES, and forward scattering experiments will be performed in line with the adsorption kinetics/TPD experiments. The ideal experimental

sequence consists of the independent adsorption of either C_2H_4 or Si_2H_6 on Si, followed by XPS, AES, forward scattering, and TPD experiments. Ideally this whole sequence would be repeated with the adsorption of a 2nd and 3rd species.

C. Results

The results to date involve the preliminary design and construction of the ultra high vacuum (UHV) system to perform the previously mentioned experiments. This system will not stand alone but will be incorporated with another UHV system already in operation (see Figure 1). This prestanding UHV system is part of the Surface Science facility at NCSU directed by Prof. Robert Nemanich. This system consists of a molecular beam epitaxy (MBE) system, an angle resolved ultraviolet photoelectron spectroscopy (ARUPS) system, and a plasma cleaning system. The UHV system for these studies will be fully incorporated into this operating system in the manner shown in Figure 1.

The AES-XPS system has been completely designed and ordered. All the equipment necessary for this system has now arrived and construction and assembly of this system will proceed immediately. The adsorption kinetics-TPD system is in the final stages of design. Most of the equipment needed for this system is already in house. As a result, the time for construction of this latter system should be greatly reduced.

D. Discussion

As a result of the desire to perform both standard XPS/AES surface experiments and forward scattering experiments, additional design criteria were required in the design of the AES/XPS system. In order to collect the AES/XPS electron intensity as a function of exit angle from the sample surface, a nonstandard manipulator with 360 degrees of rotation about two independent axes was required. The two independent rotational axes allow the electron intensity to be measured as a function of all possible departure angles. The second design criteria crucial to the ability to perform forward scattering experiments concerns the acceptance angle of the electron energy analyzer. In order for satisfactory results to be obtained, the angular acceptance of the energy analyzer must be < 2.5 degrees which is not satisfactory for most standard AES/XPS experiments with the typical acceptance angles being approximately 7-8 degrees. Therefore the energy analyzer purchased (CLAM-II from VG Microtech Ltd.) was designed to incorporate a capillary array which could be positioned to narrow the analyzers acceptance angle to approximately 1.5 degrees for forward scattering experiments and then removed for regular XPS/AES experiments.

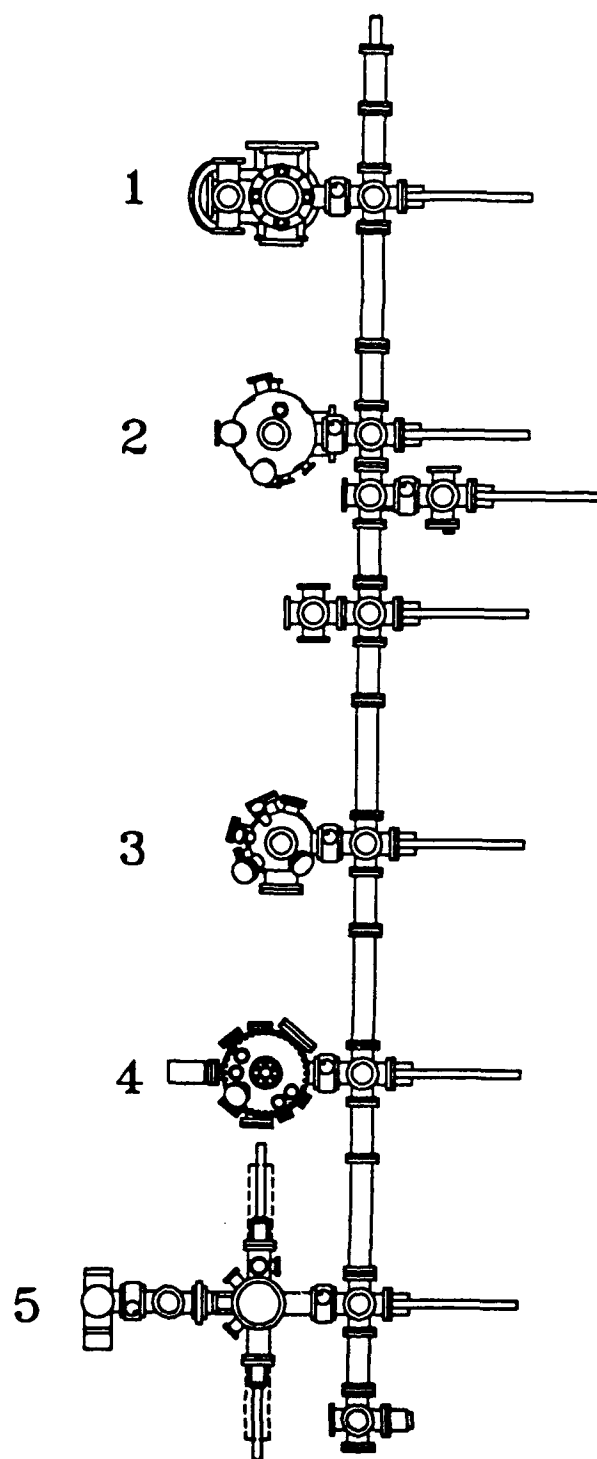


Figure 1. Schematic diagram of the ALE system incorporated with the NCSU Surface Science lab system.

1. Molecular Beam Epitaxy (MBE) system.
2. Angle resolved Ultraviolet Photoelectron Spectroscopy (ARUPS) system.
3. Auger electron/X-ray Photoelectron spectroscopy (AES/XPS) system.
4. Adsorption kinetics/Temperature Programmed Desorption (TPD) system.
5. Plasma Cleaning.

E. Conclusions

The AES-XPS system is currently under construction and should be completed by August 1992. The design of the TPD-adsorption kinetics system should be completed within a month. Assembly and construction of the TPD-adsorption kinetics system should be completed by the end of 1992.

F. Future Research Plans/Goals

Immediate goals include assembly, testing, and testing of the AES-XPS equipment. Future work will consist of the completion of the design and construction of the TPD-adsorption kinetics system.

G. References

1. J. E. Crowell, G. Lu, and B. M. H. Ning in Atomic Layer Growth and Processing, Mat. Res. Soc. Symp. Proc., vol. 222, **253** (1991), p. 1.
2. K. J. Uram and U. Jansson, J. Vac. Sci. Technol. **B7**, 1176 (1989).
3. S. K. Kulkarni, S. M. Gates, C. M. Greenlief, and H.H. Sawin, Surface Science **239**, 26 (1990).
4. Y. Suda, D. Lubben, T. Motooka, and J. E. Greene, J. Vac. Sci. Technol. **A8**, 61 (1990).
5. C. C. Cheng, R. M. Wallace, P. A. Taylor, W. J. Choyke, and J. T. Yates, J. Appl. Phys. **67**, 3693 (1990).
6. C. C. Cheng, W. J. Choyke, and J. T. Yates, Surface Science **231**, 289 (1990).
7. V. S. Smentkowski and J. T. Yates, Jr., J. Vac. Sci. Technol. **A7**, 3325 (1989).
8. A. Winkler and J. T. Yates, Jr., J. Vac. Sci. Technol. **A6**, 2929 (1988).
9. M. J. Bozack, L. Muehlhoff, J. N. Russel, Jr., W. J. Choyke, and J. T. Yates, Jr., J. Vac. Sci. Technol. **A5**, 1 (1987).
10. W. F. Egelhoff, Jr., Critical Reviews in Solid State and Materials Sciences **16**, 213 (1990).

IV. Atomic Layer Epitaxy of Diamond

A. Introduction

Atomic layer nucleation (ALN) of diamond applies the principles of atomic layer epitaxy to the initial stages of diamond nucleation. Research on ALN on non-diamond substrates has progressed steadily since the last report. We have been using both carbon species-based and metallic species-based approaches to achieve diamond nucleation on an atomic scale. A systematic and parametric investigation of carbon species-based ALN by means of DC biasing in microwave plasma enhanced CVD is near completion. The optimum parameters of biasing voltage and current as well as gas pressure have been determined. Results indicate that a diamond coating on the molybdenum substrate holder has significant effect on the diamond nucleation rate and density on a silicon substrate. Various biasing schemes are also being tested. The goal is to achieve a nucleation density approaching the theoretical limit of $10^{13}/\text{cm}^2$ assuming a critical nucleus diameter of 30 Å. Detailed results on this carbon species based ALN will be presented in the next report. Instead we will focus this report on the results we recently obtained in the carbon and metallic species based ALN approach. Hexamethyldisilane (HMDS) species have been introduced into a hot filament CVD system by either hydrogen or argon carrier gas. An organosilicic interlayer is thus formed on a single crystal silicon wafer. Experimental results of diamond nucleation on such interlayers under various nucleation and growth conditions have been obtained. The results show that such an organosilicic interlayer on a silicon substrate is promising to act as a diamond nucleation promoter. If it can be controlled at a monolayer level, the organosilicic layer can potentially be used as a direct diamond embryo for subsequent epitaxial diamond growth by the gas phase species, thus achieving the goal of atomic layer heteroepitaxial growth of diamond.

B. Experimental Procedure

1. Atomic Layer Epitaxy Chemistry of Diamond Deposition

The approach used to attaining ALN of diamond on silicon is to first deposit an organosilicic precursor epitaxially onto the silicon substrate. The organosilicics considered all contain methyl groups tetrahedrally bound to silicon that can serve as nucleation sites for diamond. Of chlorotrimethylsilane, bromotrimethylsilane, tetramethylsilane and hexamethyldisilane, HMDS was chosen as the most likely candidate since the Si-Si bond is relatively easy to break ($336.8 \text{ KJ mol}^{-1}$ compared to 435 KJ mol^{-1} for Si-C), leaving $\text{Si}(\text{CH}_3)_2$ species to adsorb onto the silicon substrate (Figure 1). The terminating layer of methyl groups are tetrahedrally oriented and can promote diamond nucleation. After the deposition of the HMDS precursor, normal diamond growth procedures utilizing hydrogen and methane chemistry hot filament chemical vapor deposition (HFCVD) is performed.

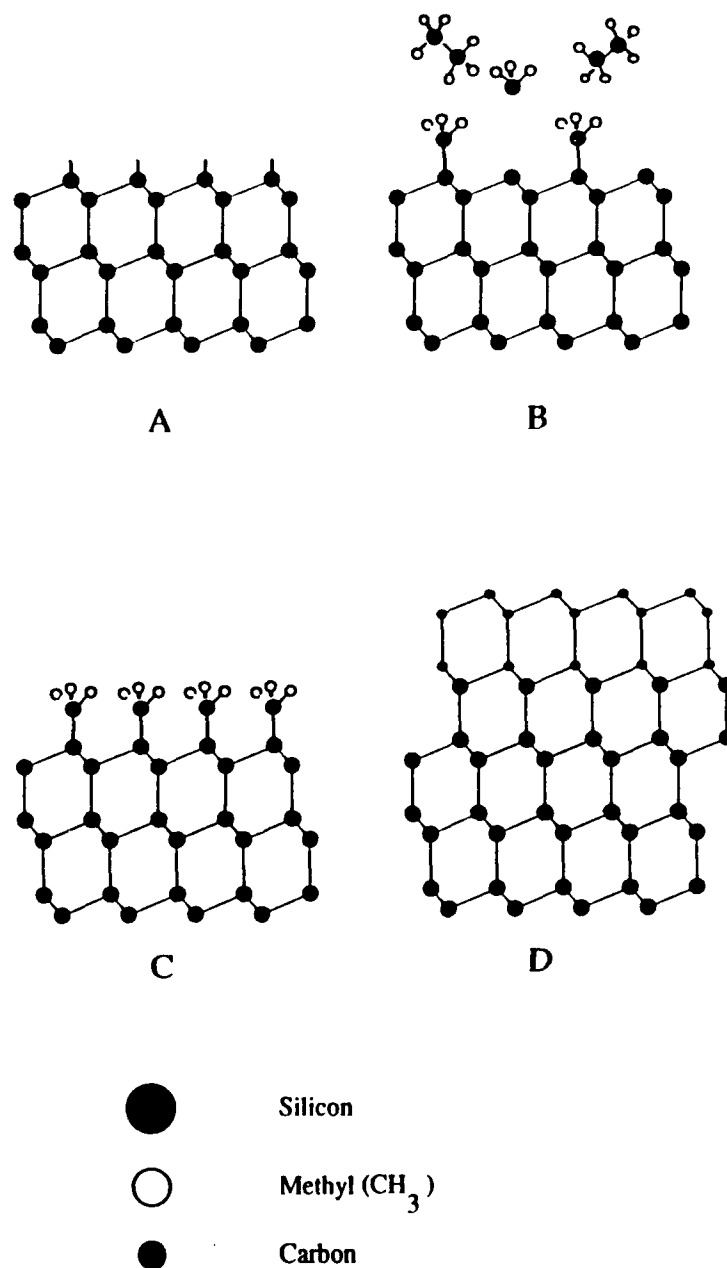


Figure 1. A model for ALN of diamond on hexamethyldisilane monolayer on Si. (A) Si surface; (B) adsorption of hexamethyldisilane precursors; (C) a monolayer of hexamethyldisilane precursors on Si; and (D) diamond nucleation and growth.

The hot filament CVD system is shown in Figure 2. A gas manifold feeds a high vacuum reaction chamber. Below the gas entry point inside the reactor are tungsten filaments positioned above a molybdenum stage. Beneath the stage is a thermocouple that measures the temperature of the underside of the substrate. The surface temperature of a sample may be as much as 100°C above the thermocouple reading. The gas flow inside the reactor is perpendicular to the surface of the substrate.

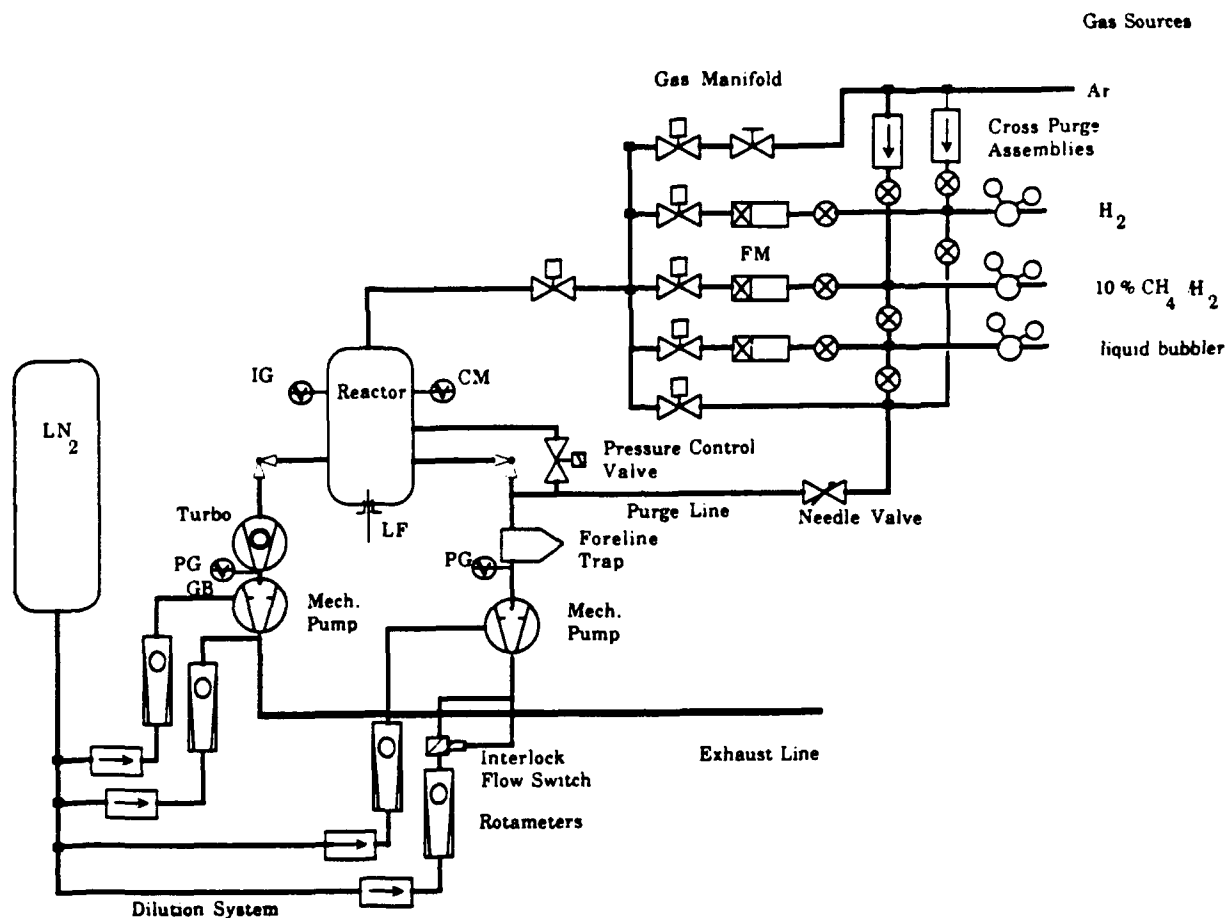


Figure 2. Schematic diagram of the HFCVD system.

2. Deposition of Organometallics

In order to deposit the organometallic liquids in precise amounts, a bubbler chamber was constructed (Figure 3) which feeds into the gas manifold of the HFCVD system. The bubbler chamber rests inside a controlled temperature bath so that the temperature and hence the vapor pressure of the liquid can be controlled. By bubbling hydrogen through the liquid with the use of micro-metering valves, controlled amounts of organometallic vapor can be admitted into the CVD reactor. The bubbler is fitted with vacuum valves and the lid has a knife edge seal so that the chamber can be pressurized in situations where a liquid with a high vapor pressure is used. A gas chromatography (GC) system in-line to the reactor gas supply is being constructed in order to be able to precisely measure the amount of organometallic delivered to the sample. We presently have to estimate the amount of exposure of the sample to the HMDS, and we have not yet been able to restrict the coverage of the sample to a monolayer of HMDS precursors.

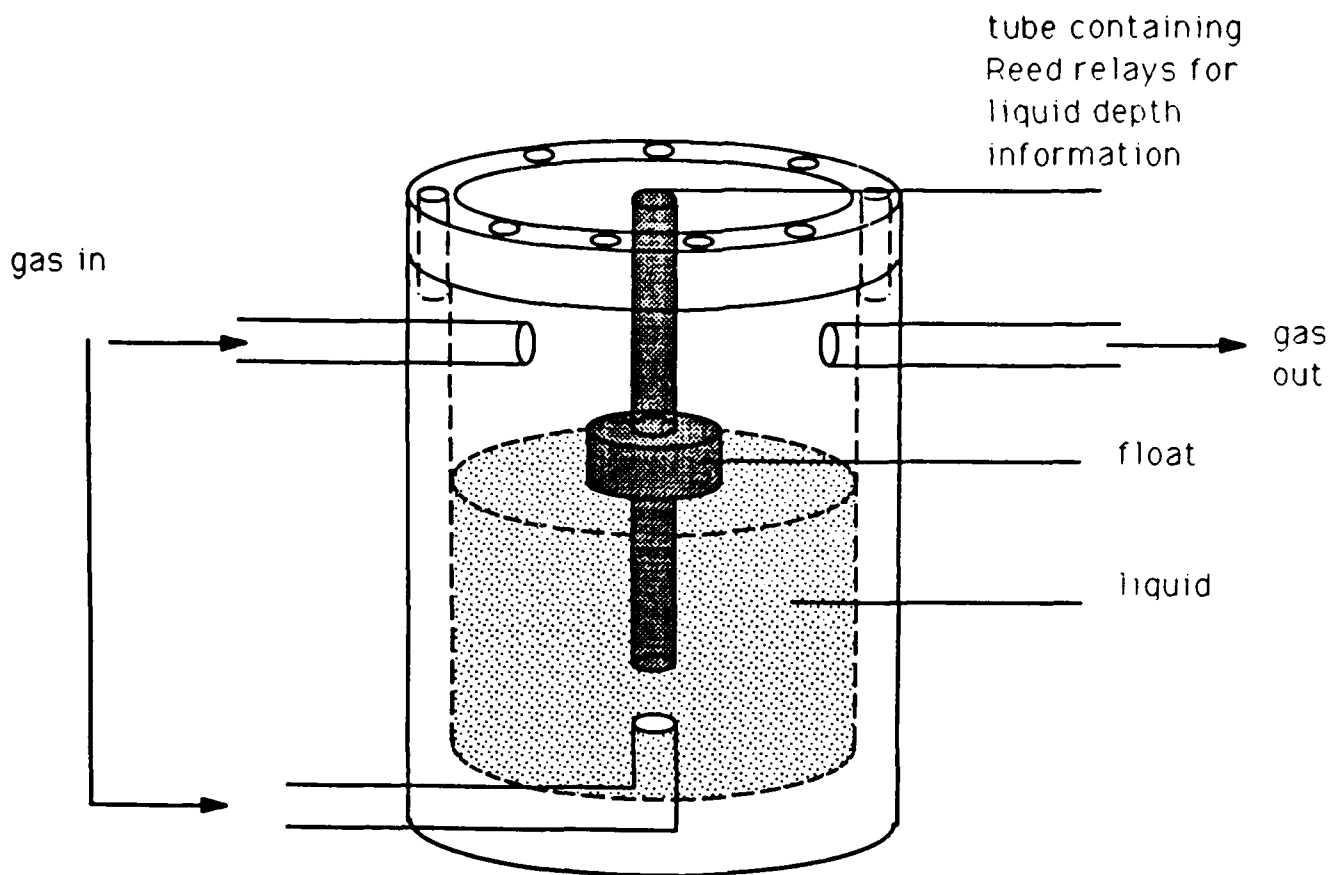


Figure 3. Schematic diagram of the bubbler.

3. Substrates

The substrates used in the experiments are <100> silicon wafers, having a diameter of one inch and a thickness of 10-12 mils. The wafers as received are etched in 10% HF to remove surface oxide, rinsed in deionized water and dried in nitrogen. They are then quickly loaded into the HFCVD reactor. The reactor is quickly brought down to 10^{-5} torr vacuum condition and left for a minimum of three hours.

4. Diamond Growth

The reactor pressure is adjusted to 30 torr while flowing pure hydrogen over the sample. The valve admitting gas from the bubbler is opened and the sample is exposed to the HMDS/H₂ vapor for the desired length of time, normally one minute. Power is then supplied to the filaments and the substrate temperature is allowed to reach 500 °C before admitting CH₄. The final substrate temperature reaches 620-680 °C.

To enhance diamond nucleation density, the substrate and filament can be biased with a DC voltage. Electrodes are attached to the molybdenum sample stage and the filament holder. During reverse biasing experiments, the substrate is negatively biased to attract cationic species from the thermal cracking of the H₂ and CH₄. During forward biasing experiments, the

substrate is positively biased to initiate electron bombardment. The biasing is performed after the substrate temperature reaches 500 °C and is performed with a methane concentration of 1% in hydrogen. The methane concentration is reduced to 0.5% after biasing for continuation of growth. The voltage between filament and substrate in forward and reverse biasing is approximately 300 V. The current ranged from 30 to 80 mA.

C. Results and Discussion

1. Interlayer Structure

After deposition of HMDS onto the substrate and during heating of the sample by the hot filament, the sample surface is seen to undergo many color changes. These color changes are due to the formation of a thin interlayer of the HMDS, the surface of which is polymerizing. The formation of this interlayer is indicative of too many layers of the HMDS pre-cursors adsorbing onto the sample surface, emphasizing the need for the GC system to allow precise measurement and thus control of the adsorption to allow monolayer coverage of the sample.

Optical microscopy reveals the existence of orthogonal cross-hatching in the interlayer structure in areas on the substrate where the interlayer has peeled away due to the high temperature of the hot filament. We believe this indicates that the interlayer is possibly ordered at the interface. The reactor presently has no *in-situ* analytical instrumentation attached, thus the samples must be removed from the reactor in order to analyze the interlayer structure. Auger spectroscopy was performed on samples exposed to HMDS but not exposed to diamond growth conditions in order to elucidate the structure of the interlayer itself. The fine structure of the carbon peak in the Auger spectrum in Figure 4 indicates the presence of sp^3 bonding in the interlayer, however, this may be due to the sp^3 bonding within methyl groups rather than to the tetrahedral orientation of the methyl groups themselves which would be favorable for diamond nucleation. X-ray Photoelectron Spectroscopy indicated the presence of silicon oxide, due to oxidation of the interlayer once the sample is exposed to air. LEED was performed in an attempt to ascertain whether the interlayer is indeed ordered at the interface with the substrate. There was no diffraction pattern observed; however, LEED is sensitive to surface contamination. The interface may be ordered while the polymerized surface is amorphous due to oxidation. X-ray Diffraction shows a small peak at a lattice spacing of 2.72 angstroms. Problems with sample oxidation and contamination currently limit the interpretation of these results and illustrate the need for *in-situ* and *in-vacuo* analytical capabilities.

2. Diamond Growth

Normal diamond growth procedure without DC bias pre treatment on <100> silicon wafers exposed to HMDS does not yield enhanced diamond nucleation density as compared to diamond growth on as-received wafers (see Figure 5). Again, since monolayer coverage of the

wafer with the HMDS precursor has not yet been achieved, the ideal epitaxial growth mechanism envisioned has not yet been tested.

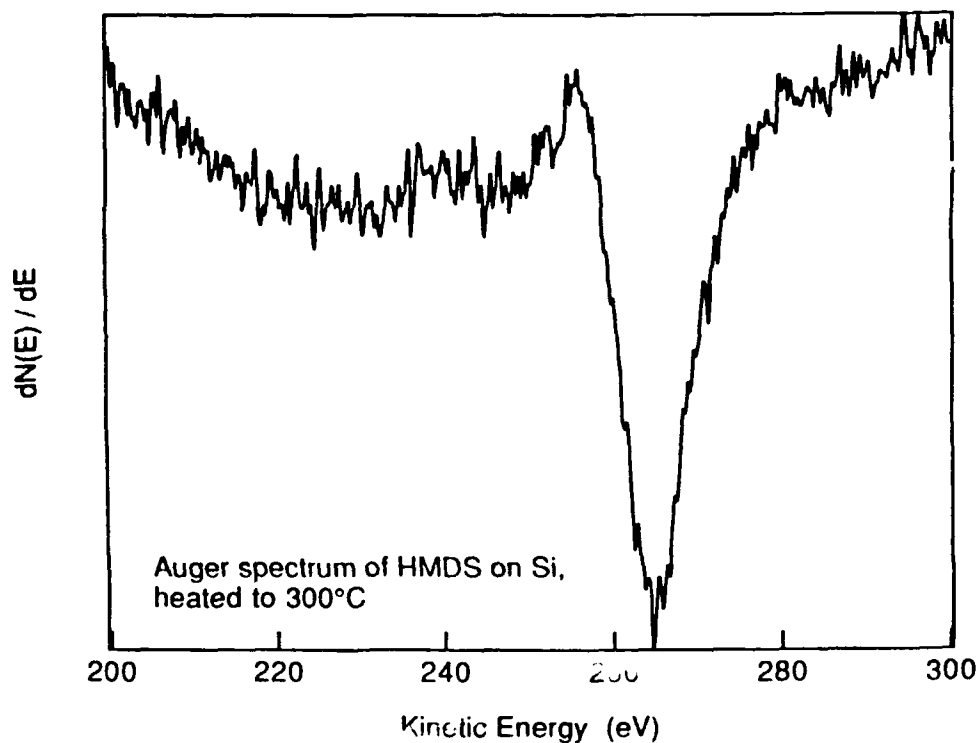


Figure 4. An Auger spectrum of the HMDS interlayer exposed to 300°C for 5 minutes.

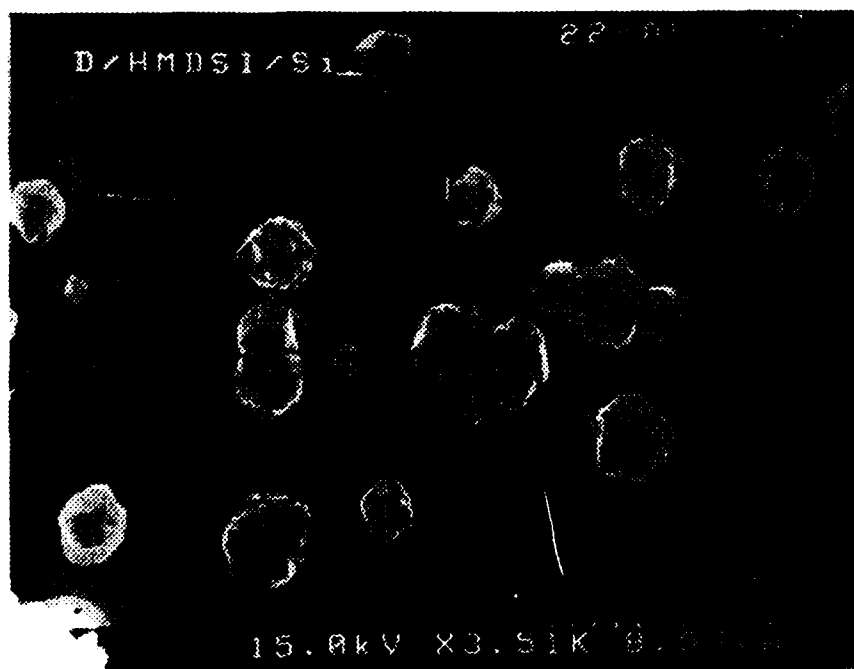


Figure 5. A SEM micrograph of diamond particles on HMDS interlayer grown without DC biasing.

Reverse bias enhanced diamond growth procedures showed massive nucleation on the HMDS interlayer as compared to as-received wafers as shown in Figure 6. The particles did not appear to grow larger, and constant re-nucleation might be occurring at the surface. A micrograph of an area on a wafer exposed to HMDS where a hole exists in the interlayer is seen in Figure 7. It is observed that the nucleation on the interlayer is much greater than that on the bare substrate surface. Raman spectroscopy of these particles revealed a broad peak at 1332 cm^{-1} , indicative of diamond like carbon (see Figure 8). There is also a graphitic peak at 1600 cm^{-1} . An unknown peak at 1122 cm^{-1} is probably due to a disordered structure. Since the HMDS interlayer is many layers thick it is believed that there is too high a carbon concentration at the substrate surface leading to poor diamond quality. Reducing the biasing time or the methane concentration may improve the diamond quality in future experiments. We have also conducted forward biasing experiments which resulted in electron bombardment on the HMDS interlayer. The HMDS interlayer became granular after electron bombardment. The exact nature of this electron bombardment and its effect to the interlayer structure remains to be investigated.

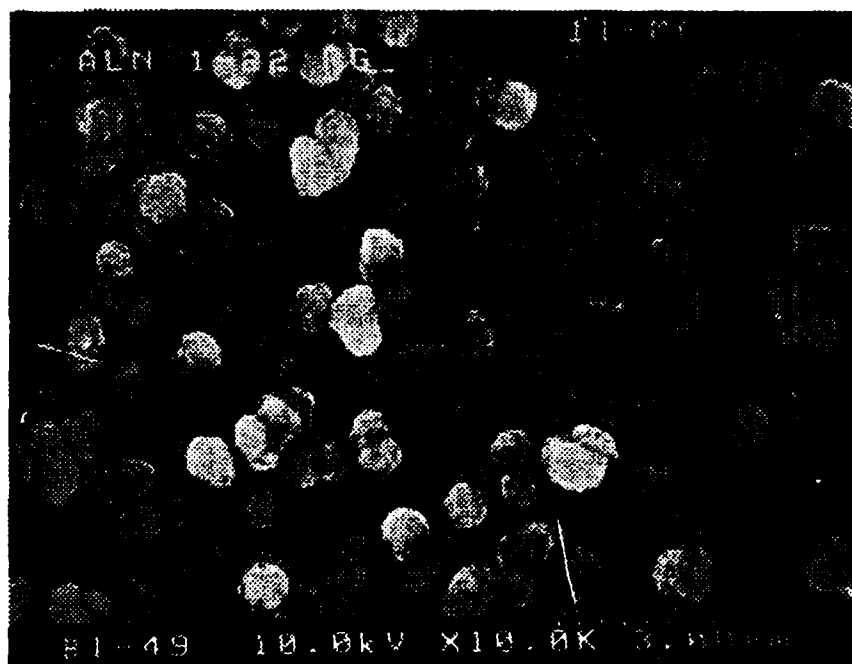


Figure 6. A SEM micrograph of diamond like particles grown on HMDS interlayer using reverse dc biasing for a period of 10 hours.

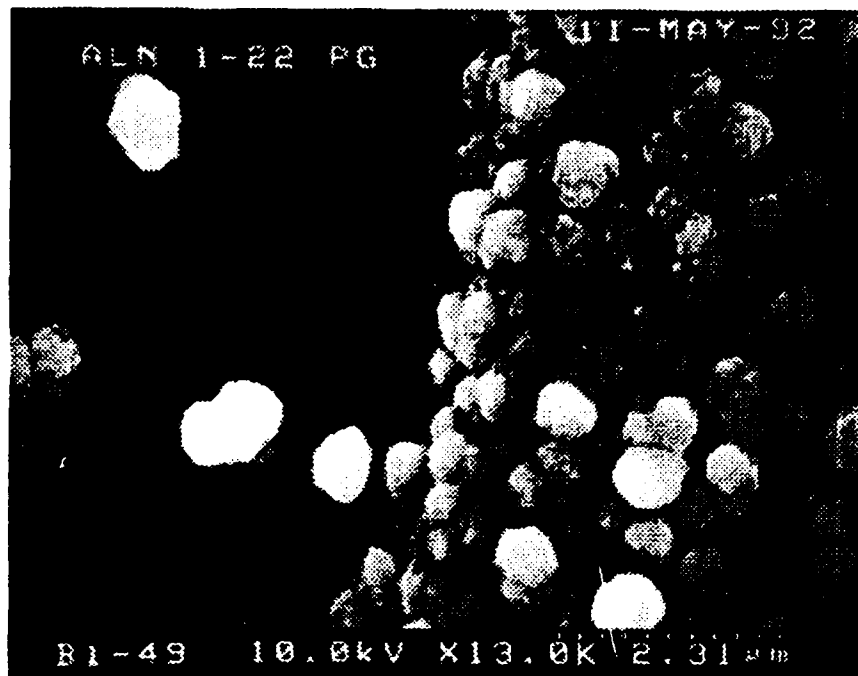


Figure 7. A SEM micrograph illustrating the difference in nucleation densities on HMDS compared to bare Si surface.

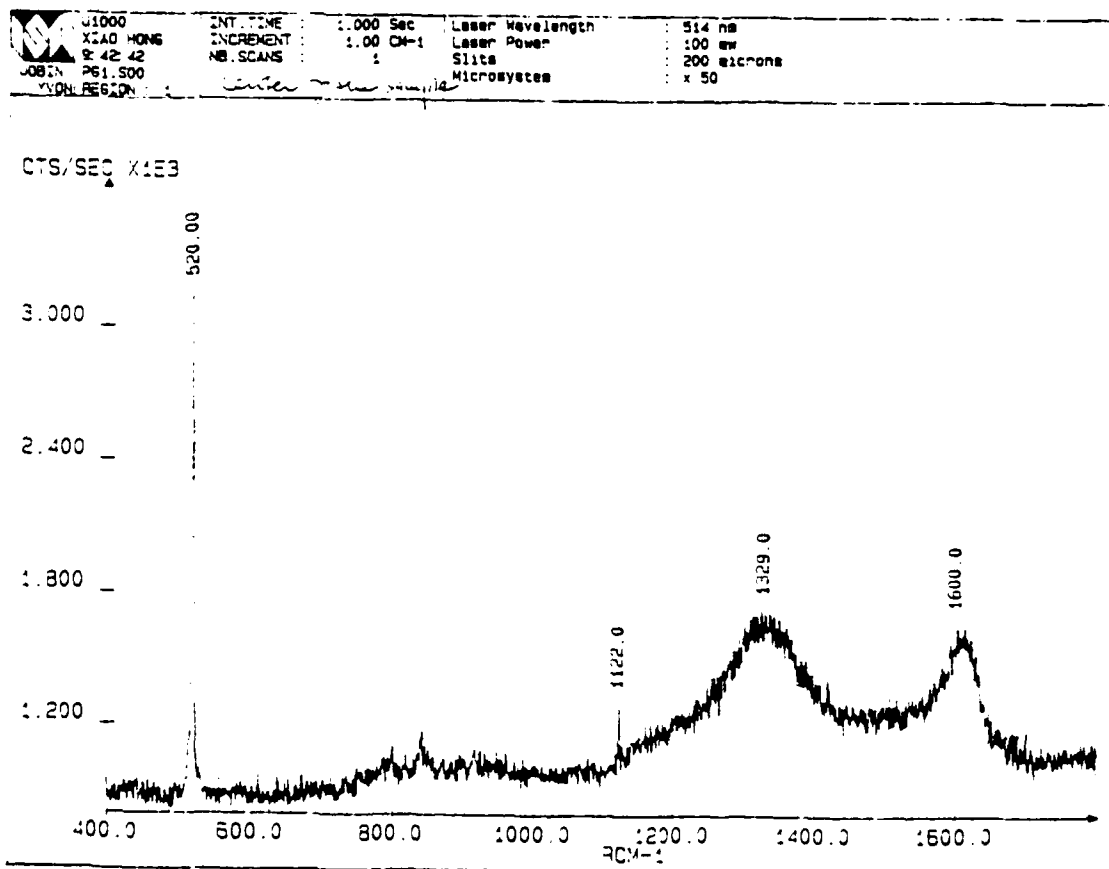


Figure 8. A Raman spectrum of the diamond-like particles.

D. Conclusions

Organosilicic interlayers have been successfully deposited onto single crystal silicon surfaces. Subsequent diamond nucleation and growth has been conducted. It was found that reverse biasing on the HMDS interlayer results in significant enhancement of nucleation. The HMDS interlayer itself may directly convert to diamond structure if the deposition can be controlled at monolayer levels. Results indicate that the HMDS layer has great potential in promoting heteroepitaxial diamond nucleation and growth on silicon.

E. Future Research Plans/Goals

We will further investigate the organosilicic species in more detail. The near term goals are to understand the interlayer structure, control the interlayer thickness to monolayer range, and nucleate and grow diamond on the surface of such layers at high densities and hopefully in an oriented fashion. We are currently setting up an *in-vacuo* ESD and XPS analytical system that is directly coupled to the HFCVD growth system so that the interlayer can be analyzed without contaminants from the air. Direct TEM and transmission electron diffraction will also be conducted to characterize the layer structure. We will use gas chromatography (GC) to measure the concentration of organosilicic species in the gas phase; thus enabling us to control the amount of organosilicic species adsorbed to a monolayer. In addition to the HMDS, other species such as tetramethylsilane and trimethylborate will also be tested. Experiments including direct conversion of the organosilicic layer under atomic hydrogen atmosphere, a study of nucleation density as a function of biasing time and growth time, and independent temperature control of the substrate using a water cooling stage will be performed.

V. Epitaxial Growth of CeO₂ on Si

A. Introduction

The growth of epitaxial ceramic thin films on silicon is of interest for applications to high quality silicon-on-insulator (SOI) layers and stable capacitor devices. CeO₂ is an excellent candidate for such an insulator, having the cubic fluorite structure, with the lattice misfit factor $\Delta a/a$ for CeO₂ to Si being 0.35% [1]. Also, CeO₂ has a dielectric constant of ~26, which could potentially allow it to be used in stable capacitor devices of small dimensions.[1]

B. Experimental Procedure

1. Silicon Wafer Cleaning

In order to achieve epitaxial growth, one must start with an atomically clean substrate. To this end, a three-step surface preparation technique is being developed [6]. In the first step, the silicon substrate is irradiated with ultra-violet light in an oxygen ambient. This UV/Ozone cleaning causes contaminant molecules to react with atomic oxygen, forming volatile molecules such as CO₂, H₂O, N₂, etc..[6] At the same time, a thin layer of SiO₂ is formed on the surface of the wafer. Figure 1 shows the UV/Ozone cleaning apparatus that has been constructed. The second step is a wet chemical etch in dilute HF, which serves to remove any oxide on the wafer, and leaves a hydrogen-terminated surface. Finally, the substrate may be heated up to 1000°C under ultra-high vacuum to desorb any contaminants acquired between the chemical etch and insertion into the chamber. These three steps combine to provide an atomically clean surface necessary for epitaxial growth.

2. Thin Film Deposition

It has been shown that crystalline layers of CeO₂ may be grown on a Si substrate by means of laser ablation [2,3]. This process can be accomplished by irradiating a solid CeO₂ target with a high energy pulse from an excimer laser under ultra-high vacuum (UHV). This produces a "plume" of CeO₂ molecules free to move in UHV and form epitaxial layers on the Si substrate. By controlling the frequency and length of the pulses of laser, one hopes to achieve layer by layer growth of the oxide.

In order to maintain stoichiometry of CeO₂ in UHV, it is believed that it is necessary to flow oxygen at low pressure (10^{-7} – 10^{-8} torr) during growth [1,2]. Ce, however, has a high oxygen affinity and x in CeO_{2-x} has been reported to be less than 0.01 at 1000° C under 7.6×10^{-9} torr oxygen, indicating that oxygen flow may be unnecessary [3,4].

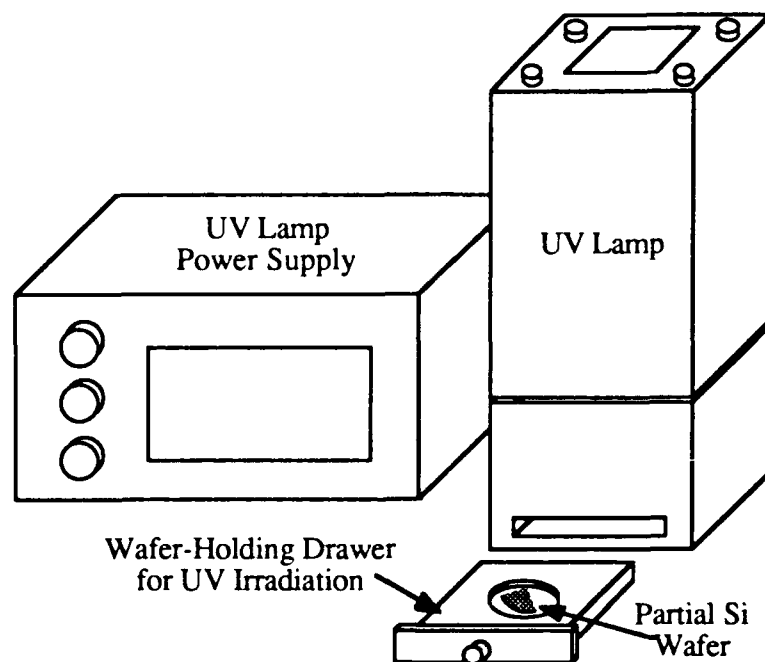


Figure 1. Diagram of existing UV/ozone cleaning system.

3. Characterization of Thin Films

In order to observe quality, crystallinity, orientation, and growth rate of CeO_2 on Si, *in situ* reflection high energy electron diffraction (RHEED) will be used. A quadrupole mass spectrometer (QMS) will be used to detect residual gases and observe the oxidation state of the ablated CeO_{2-x} . Base pressure in the reaction chamber will be measured by an ion gauge. *Ex situ* characterization methods will include transmission electron microscopy (TEM) and x-ray diffraction. For characterization by x-ray diffraction, we are considering adding a new sample holder to our high resolution double crystal diffractometer. This addition will enable us to perform grazing incidence diffractometry. This sample holder and the present channel cut collimator will upgrade our capability for x-ray characterization of ultra-thin films.

C. Results

A design has been developed and a system suitable for growing epitaxial CeO_2 on Si is under construction. This system consists of 3 chambers: a load-lock entry chamber equipped with a 60 l/s turbomolecular pump, an intermediate chamber with a de-gas station, evacuated by a 220 l/s ion pump, and the main chamber for oxide deposition using a 400 l/s ion pump. A 300 l/s turbomolecular pump may be added to the deposition chamber later, if oxygen flow is deemed necessary. The three chambers are linked in such a way that the growth chamber is never open to a chamber that is exposed to atmosphere. In this fashion the strict requirement of ultra-high vacuum in the deposition chamber can be met. Figure 2 shows a side view of the

system arrangement. The laser to be used is a Lamda Physik excimer laser, currently available in the laboratory.

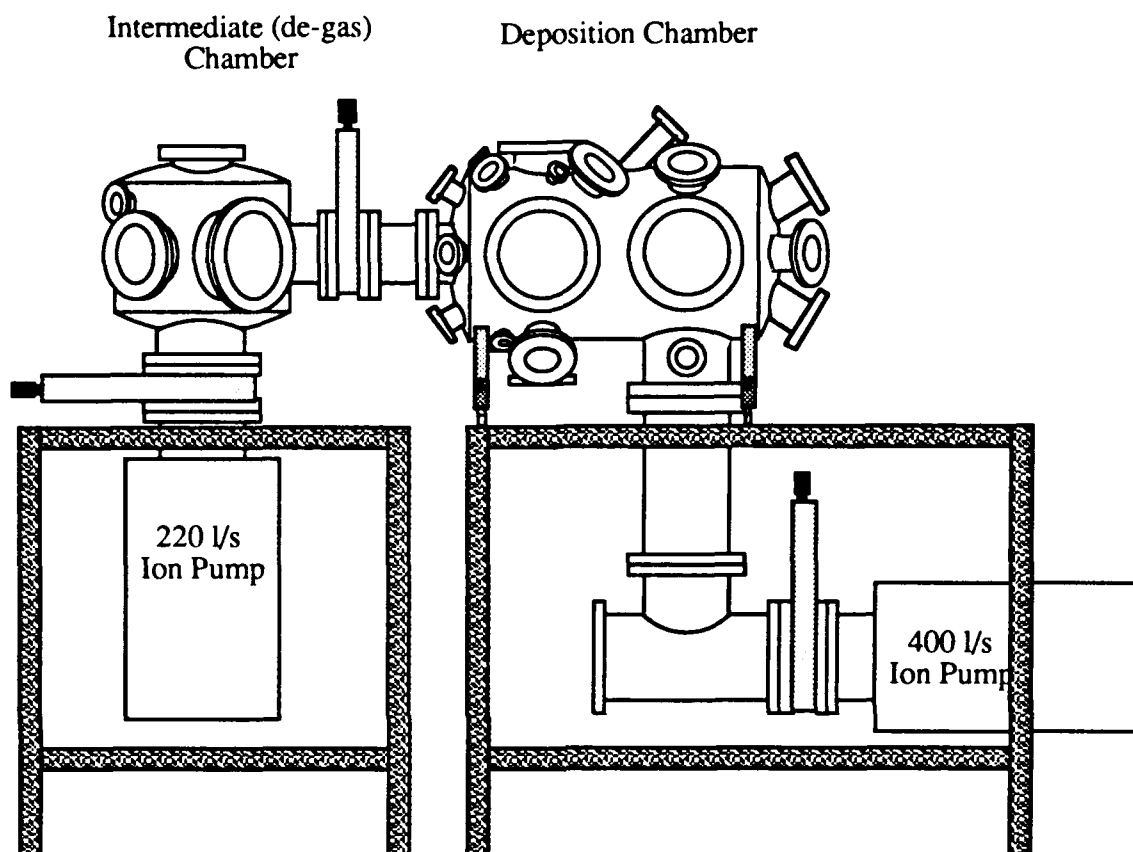


Figure 2. Side view of vacuum chambers for growth of CeO_2 .

The substrate holder and transport mechanisms will have a 2" diameter substrate capacity. The internal manipulator will provide 360° continuous rotation. For this design the substrate platen will be facing down, and the sample held in place by clips. Also, heating up to 1000° C will be provided by an oxygen-resistant quartz lamp within the manipulator. The manipulator will have 2" of vertical motion to allow the target to substrate distance to vary.

D. Discussion

Some progress has been made for the CeO_2 system, however, we have been delayed due to the lack of available laboratory space. A new place to put this equipment has been arranged, but it involves some major reconstruction of the laboratory. The university is now acting on our building requests, and these renovations should be completed in July. Figure 3 shows a picture of the hardware assembled to date, in a temporary space.

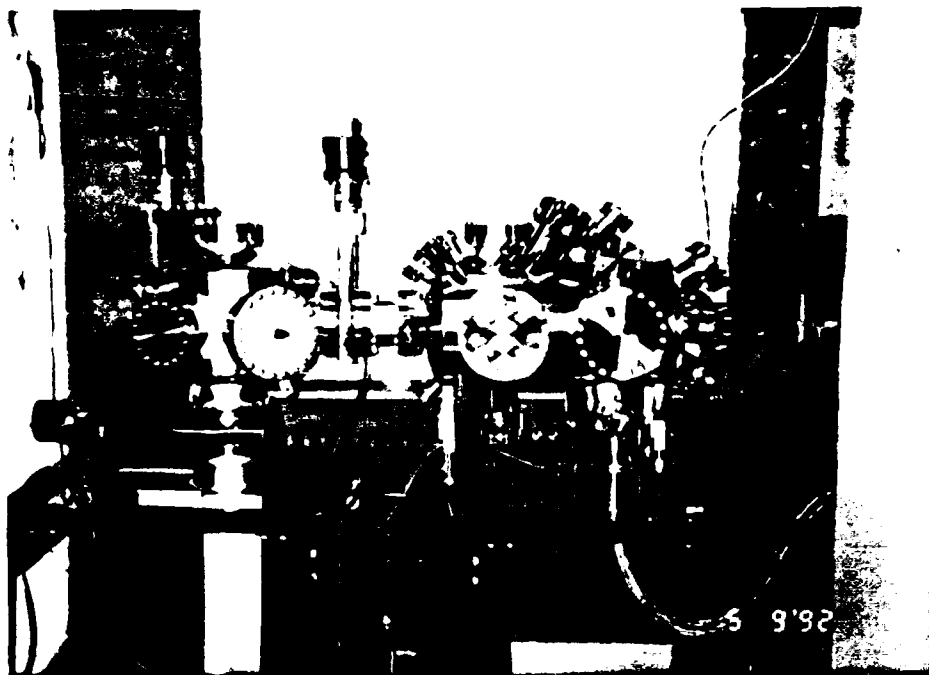


Figure 3. Picture of CeO₂ deposition system.

E. Conclusions

The system for epitaxial growth of cerium oxide is currently under construction. The system will be functional in 1992.

F. Plans for Future Work

Immediate plans include building the system and depositing oxide.

G. References

1. T. Inoue, Y. Yamamoto, S. Koyama, S. Suzuki, and Y. Ueda, *Appl. Phys. Lett.*, **56**, 1332 (1990).
2. M. Yoshimoto, H. Nagata, T. Tsukshara, and H. Koinuma, *Jpn. J. Appl. Phys.*, **29**, L1199 (1990).
3. H. Koinuma, H. Nagata, T. Tsukshara, S. Gonda, and M. Yoshimoto, *Extended Abstracts of the 22nd Conference on Solid State Devices and Materials*, Sendai, Japan, 1990, p. 933.
4. O. T. Sørensen, *J. Solid State Chem.* **18**, 217 (1976).
5. C. N. Afonso, R. Serna, F. Catalina, and D. Bermejo, *Appl. Surf. Sci.* **46**, 249 (1990).
6. P. Tiwari, "In-Situ Laser Processing of High T_c Superconductor and Semiconductor Heterostructures" Doctorate Thesis, Dept. of Materials Science and Engineering, NCSU, 1991.

VI. Distribution List

	Number of Copies
Mr. Max Yoder Office of Naval Research Electronics Division, Code: 1114SS 800 N. Quincy Street Arlington, VA 22217-5000	3
Administrative Contracting Officer Office of Naval Research Resident Representative The Ohio State University Research Center 1314 Kinnear Road Columbus, OH 43212-1194	1
Director Naval Research Laboratory ATTN: Code 2627 Washington, DC 20375	1
Defense Technical Information Center Bldg. 5, Cameron Station Alexandria, VA 22314	12